Variable Stiffness Treadmill (VST): System Development, Characterization, and Preliminary Experiments

Jeffrey Skidmore, Andrew Barkan, and Panagiotis Artemiadis

***Abstract*—Locomotion is one of the human's most important functions that serve survival, progress, and interaction. Gait requires kinematic and dynamic coordination of the limbs and muscles, multisensory fusion, and robust control mechanisms. The force stimulus generated by the interaction of the foot with the walking surface is a vital part of human gait. Although there have been many studies trying to decipher the load feedback mechanisms of gait, there is a need for the development of a versatile system that can advance research and provide new functionality. In this paper, we present the design and characterization of a novel system, called variable stiffness treadmill (VST). The device is capable of controlling load feedback stimulus by regulating the walking surface stiffness in real time. The high range of available stiffness, the resolution and accuracy of the device, as well as the ability to regulate stiffness within the stance phase of walking, are some of the unique characteristics of the VST. We present experiments with healthy subjects in order to prove the concept of our device and show preliminary findings on the effect of altered stiffness on gait kinematics. The developed system constitutes a uniquely useful research tool, which can improve our understanding of gait and create new avenues of research on gait analysis and rehabilitation.**

***Index Terms*—Medical control systems, medical robotics, rehabilitation robotics.**

I. Introduction

STIMULUS is a vital part of human gait and is the feedback that governs the way we operate in our complex and evolving environment. In human gait motion, there are many forms of stimulus. However, each type of stimulus holds essential information, without which, proper gait motion would be an impossible task. While the effect of load feedback (an important stimulus) on gait has been an active field of study (see, for example, [1]–[9]), there is a need for the development of a versatile system that can advance research in this area by providing new functionality.

In previous studies, researchers have utilized compliant surfaces to investigate the effect of load feedback on gait. The simplest setups include surfaces created out of foam of varying stiffness [10], [11] or collegiate gym mats [12]. However, inherent in these setups is the inability to utilize a large range of stiffness while maintaining high resolution—without employing an extreme number of materials.

The development of devices that allow for easy adjustment of stiffness between experiments began decades ago with McMahon and Greene [13]. Their setup included simply supported plywood boards where the stiffness is changed by adjusting the distance between the two supports [13]. More recently, Kerdok *et al.* also utilized the concept of the deformation of a supported compliant beam in their development of a compliant track treadmill [14]. While improving the easiness and resolution of compliant walking surfaces, these designs do not allow for the compliance of the surface to be changed *in situ*. Moreover, there is no ability to exert a prescribed force perturbation to the foot in real time while a subject is actively walking on the surface.

In order to address the gaps left by other devices, a novel system, called variable stiffness treadmill (VST), has been developed with several advantages over existing devices. First of all, the VST has a wide range of controllable stiffness—theoretically zero to infinite, but maintains high resolution. Second, it has the ability to actively vary and control the compliance of the treadmill surface within the gait cycle. Unlike previous devices, the VST is capable of creating any profile of stiffness during an experiment and throughout the gait cycle. Third, by measuring the displacement of the walking surface, we can not only estimate the load force exerted on the foot, but can also exert a force on the foot by adjusting the stiffness in real time. The above elements create the potential for better understanding of gait. The novel setup we have developed allows for a large range of selectable stiffness throughout the gait cycle, as well as for full-continuous control of that stiffness during the stance phase. This makes it possible to introduce a plethora of force perturbations to the leg that are impossible to implement with current devices. Since force stimulus and joint displacement are such important sources of feedback for human gait, it is hypothesized that perturbations of surface stiffness to the gait cycle will elicit changes in kinematic patterns and muscle activations that might yield meaningful conclusions about human gait mechanisms.

The variation of stiffness also results in the ability to recreate the stimulus of compliant surfaces for the purpose of simulating environments. Vertical stiffness control gives operators the opportunity to test artificial walkers for efficiency and robustness by introducing surface stiffness disturbances to their gait. For these reasons, the VST has the potential to be used by researchers in the field of motor and gait rehabilitation as an investigative or rehabilitation instrument. Additionally, gait trainers can use

Manuscript received May 26, 2014; accepted August 3, 2014. Date of publication September 11, 2014; date of current version August 12, 2015. Recommended by Technical Editor S. Q. Xie.

The authors are with the School for Engineering of Matter, Transport and Energy, Arizona State University, Tempe AZ 85287 USA (e-mail: jaskidmo@asu.edu; abarkan@asu.edu; panagiotis.artemiadis@asu.edu).

Color versions of one or more of the figures in this paper are available online at http://ieeexplore.ieee.org.

Digital Object Identifier 10.1109/TMECH.2014.2350456

the system as an environment simulator for exercise or motor replication scenarios. The unique capabilities of the VST can also be utilized to measure the active impedance of the lower limbs by applying controlled perturbations to the ankle joint during the stance phase.

In this paper, we introduce the VST system by presenting its design characteristics and closed-loop performance, and the results of initial experiments. We first present the concept of variable stiffness and the mechanism used to control it, followed by its closed-loop performance. Then, we analyze the subsystems of the total device that allow for its real-time operation. Experiments with human subjects were designed in order to prove the concept of our device. We present experimental data that show the efficiency of the system and preliminary data on the effect of variable body weight support and low stiffness perturbations on gait kinematics. The proposed system constitutes the first mechanical device that can alter the walking surface stiffness in real time, with high accuracy, resolution, and robustness. The latter characteristics provide a uniquely useful research tool, which can improve our understanding of gait and create new avenues of research on gait analysis and rehabilitation.

The rest of the paper is organized as follows. Section II details the structure of the device along with its technical specifications and provides characterization of the system. Section III presents proof-of-concept experiments using the VST with healthy subjects. Finally, Section IV concludes the paper with a brief discussion and summary of the contribution.

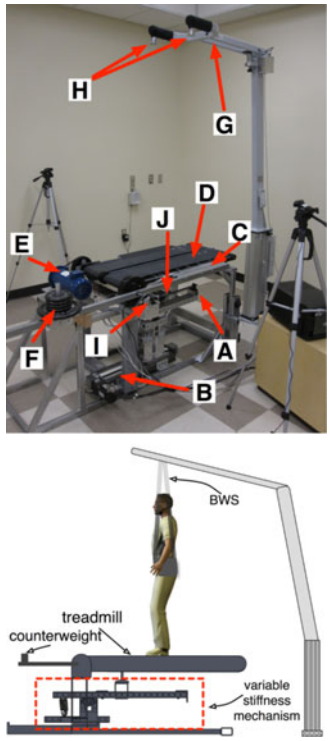

Fig. 1. VST setup. Actual platform (top) and conceptual diagram (bottom). Subsystems shown include: A) Variable stiffness mechanism, B) Linear track, C) Force sensor mat, D) Split treadmill, E) Treadmill motor, F) Counter-weight system, G) Custom-made harness-based body-weight support, H) BWS load cells, I) Rotary encoder for treadmill inclination measurement, J) Load cell for walker foot force measurement.

II. Methods

A. Design Characteristics

The VST achieves greater versatility and functionality than other devices by combining a variety of components into one unique system. The device is shown in Fig. 1. The major components of the VST include a variable stiffness mechanism, a linear track (Thomson Linear Inc), a force sensor mat, a split belt treadmill, a DC treadmill motor (Anaheim Automation), a counter-weight system, and a custom-built body weight support (LiteGait) with two load cells that measure the weight of the subject being supported by the system. Each component is important to the system for the overall function and proper investigation of gait and will be analyzed below.

B. Variable Stiffness Mechanism

The main novel feature of the VST is the ability to vary the vertical stiffness of the walking surface (i.e., treadmill), therefore controlling the kinetic and kinematic interaction between the walker and the walking surface. The capability of the VST to achieve a large range of controllable stiffness with high resolution comes from a novel variable stiffness mechanism. In its most simplified form, the variable stiffness mechanism is a spring-loaded lever mounted on a translational track, as shown in Fig. 2. The effective stiffness of the treadmill, located at a distance x from the pivot joint, is dependent on the coefficient of stiffness S of the linear spring and the moment arm r through which it exerts a force [15]. By design, S and r remain constant, therefore, the effective stiffness of the treadmill can be controlled by changing the distance x.

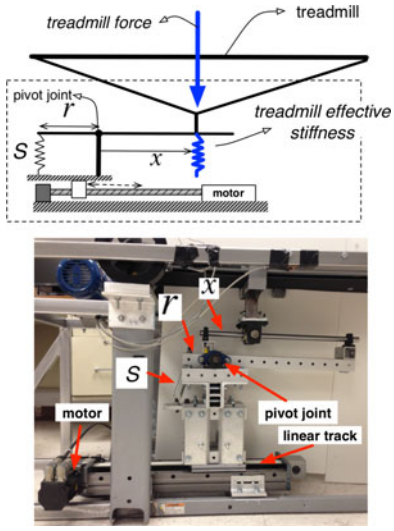

Fig. 2. Variable stiffness mechanism. Conceptual diagram (top) and actual setup (bottom).

In order to achieve our desired range of stiffness, we built the variable stiffness mechanism (see Fig. 2) with two extension springs of stiffness $k = 5122$ N/m, rest length $l_0 = 12.7$ cm, and

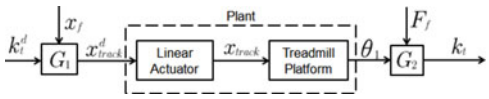

Fig. 3. Block diagram of the open-loop system.

outside diameter $OD = 2.54$ cm (LE 135J 06 M, Lee Spring Co.). The two springs are combined in parallel, and are attached to the lever arm at a distance of 7.5 cm from the pivot point. The spring stiffness was chosen to meet our specification for the range of effective treadmill stiffness, which is analyzed below.

This entire assembly sits on the carriage of a high-capacity linear track (Thomson Linear, Part Number: 2RE16-150537) which is controlled by a high-precision drive (Kollmorgen, Part Number: AKD-P00606-NAEC-0000) and has a translational resolution of 0.01 mm. This results in a high resolution for the adjustment of effective stiffness, which is discussed below.

In addition to achieving the desired range and resolution of stiffness with the variable stiffness mechanism, we can also vary the treadmill stiffness actively throughout the gait cycle. In the most extreme scenario of going from a rigid surface, i.e., treadmill stiffness of $k_t = \infty$, to the minimum achievable stiffness, the linear track will have to move across its entire range (0 to 0.40 m). Considering that the linear track can move as fast as 3 m/s, the system could make this extreme change in stiffness in 0.13 s. Assuming that the subject is walking at a normal pace of 1.4 m/s [16], [17], with a stride length (the distance between consecutive points of initial contact by the same foot) of 1.4 m [18], the stance phase would last approximately 0.5 s. This means that the variable stiffness mechanism can make this extreme change in stiffness three times during the stance phase. Therefore, it can easily change stiffness many times throughout the gait cycle when the desired change in stiffness is smaller than the two extremes. The ability to change stiffness at a high rate throughout the stance phase of the gait cycle adds to the unique capabilities of the VST.

C. System Modeling

The relationship between a desired stiffness and the actual effective stiffness of the treadmill is described by the governing equations of the system and the plant dynamics. The system is displayed in block diagram form in Fig. 3 where the desired treadmill stiffness (k_t^d) is the reference signal, the desired linear track position (x_{track}^d) is the control input, the angular deflection of the treadmill (θ_1) under an applied load is the result of the track movement, and the actual-measured stiffness (k_t) is the final output. The open-loop transfer functions (G_1, G_2) are relationships between variables of the system and are determined by the governing equations. The plant is the combination of the dynamics of the linear actuator and the treadmill platform. The governing equations have been discussed previously [19], so only the dynamics of the system are discussed below.

1) Plant Dynamics: The dynamics of the system are governed by the combined dynamics of the linear actuator and the treadmill platform. The dynamics of the linear actuator are observed to be very fast compared to the treadmill. More specifically, the linear actuator is able to reach the desired position in approximately 20 ms, with a steady-state error less than 0.01 mm. Therefore, we assume that the dominant open-loop poles will be given by the dynamics of the treadmill. While our system operates in discrete time, we model it here in continuous time to demonstrate some important characteristics of the system. Approximating the treadmill with second-order dynamics, the final open-loop transfer function between the actual and desired treadmill stiffness is given by

$$\frac{K_t(s)}{K_t^d(s)} = G_1 G_2 \frac{K}{s^2 + 2\zeta\omega_n s + \omega_n^2}. \tag{1}$$

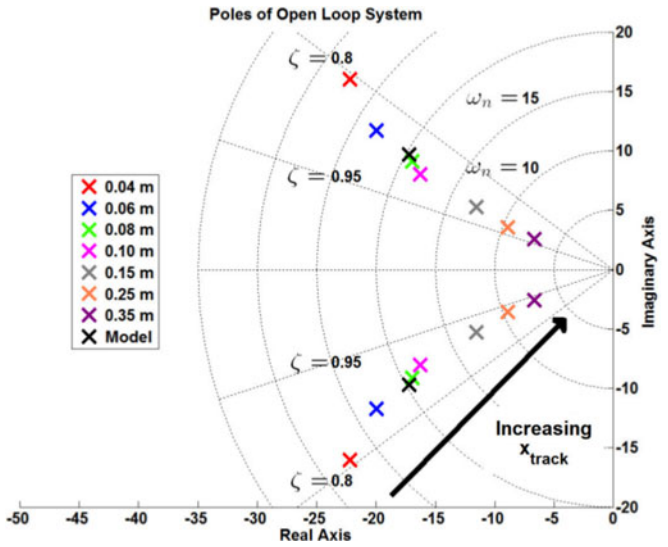

Fig. 4. Plot of the open-loop poles for different x_{track} positions in the s-plane.

Although the system has been represented so far as linear—therefore, the use of transfer function, our system is actually nonlinear, since the value of K, as well as the damping ratio and natural frequency of the system will change as the input x_{track} changes. In other words, since we are using the input x_{track} to change the effective stiffness of our treadmill, the dynamics of the treadmill will change for different values of x_{track}. This will in turn change the pole locations of the system. Therefore, a linear model will not accurately describe this system for its entire range of stiffness. To understand the nonlinearity of the system and the effect of changing the stiffness, we found the open-loop poles at a variety of x_{track} positions and plotted them in the s-plane shown in Fig. 4.

The poles were found by identifying key parameters from the step response of the system. A known mass of 11.71 kg was placed at 0.33 m from the pivot point, and x_{track}^d was suddenly changed from 0 to an arbitrary value. The angular deflection of the treadmill was measured with an encoder to find the second-order system response. The damping ratio (ζ)

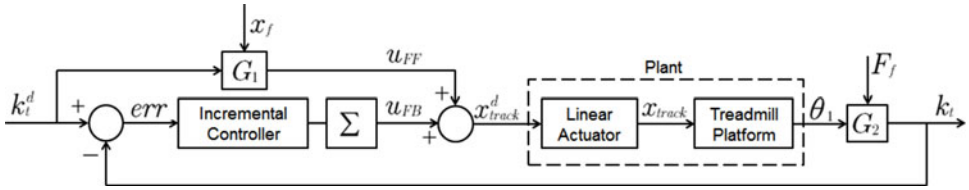

Fig. 5. Block diagram of closed-loop system.

was calculated from the maximum overshoot and the undamped natural frequency (ω_n) was calculated from the damped natural frequency and the rise time of the step response. The poles of the system were finally calculated by solving for $s_p = -\zeta\omega_n \pm j\omega_n\sqrt{1-\zeta^2}$.

Based on the pole locations in the s-plane, we find that the system is highly damped ($\zeta > 0.8$) and has a quick response (rise time: $t_r \leq 0.25$ s) for all track positions. As x_{track} increases, the damping ratio also increases and the natural frequency decreases. The variability of the pole locations with changing stiffness prevents us from describing the entire system with one linear model. However, the above analysis gives an overview of the dynamics of the system.

2) Linear Model: We chose to create a linear model about a reference input of $k_t^d = 20$ kN/m to further investigate the dynamic response of the system. We chose $k_t^d = 20$ kN/m because it is a stiffness that is similar to other studies that have been performed [20]–[22], and because we expect to use primarily values of stiffness of this range in future experiments. The linear model was identified by placing a known mass (11.7 kg) at a constant distance (0.33 m) from the treadmill pivot point, and commanding a step input by holding the desired stiffness at 2 MN/m and then suddenly dropping it to 20 kN/m. This corresponds to x_{track}^d changing from 0 to 0.065 m. This resulted in a damping ratio of $\zeta = 0.87$ and natural frequency $\omega_n = 19.74$ rad/s. By creating a bode plot based on the transfer function calculated from these system parameters, the system bandwidth frequency (defined here as the first frequency where the gain drops below -3 dB of its DC value) for the linear model is 2.45 Hz.

The identified linear model is useful for understanding the treadmill system but, as shown above, is not sufficient for controlling the stiffness of the treadmill due to inherent nonlinear relationships of the system. However, the errors in the linear model can be reduced by implementing a feedback control law. Implementing a proportional integral (PI) feedback controller will not only allow us to shape the transient dynamics and drive the steady-state error to zero, but the PI controller will also compensate for the nonlinearities that are neglected by the linear model.

D. Closed-Loop System Characterization

A PI feedback controller was designed and implemented in order to achieve a zero steady-state error of the actual treadmill stiffness in response to a desired stiffness reference signal. A block diagram representing the closed-loop system is shown in Fig. 5 where err is the error signal and u_{FF} and u_{FB} are the feedforward and feedback control efforts, respectively. The transfer function G_1 is the same as described previously and is placed in the feedforward path to get the control input close to its final value. The feedback controller then makes the corrections necessary to eliminate the steady-state error. The actual stiffness is calculated based on the force exerted by the walker on the treadmill (F_f in the block diagram) and the actual vertical displacement of the treadmill, computed through the rotary encoder measurements (θ_1). The walker force F_f is measured in real time via a 500-kg S-type load cell (RobotShop, Product Code: RB-Phi-204) mounted between the treadmill platform and the variable stiffness mechanism, as shown in Fig. 1 (part J).

The design of the PI controller was performed in the continuous-time domain by placing poles in the s-plane to decrease the rise time of the response and eliminate the steady-state error. The control law was implemented in the discrete time domain with an incremental or velocity algorithm [shown in (2)], where err^p is the error calculated at the previous sample, k_p and k_i are the P and I gains, respectively, and Δt is the sample period.

$$\Delta u_{\text{FB}} = k_p\left(err - err^p\right) + k_i err \Delta t. \tag{2}$$

This change in feedback control effort is summed over time and results in the desired track position when added to the feedforward control. The proportional and integral gains were tuned to the linear model and then reduced to compensate for the implementation in discrete time instead of continuous time.

The feedback control structure was validated with two different reference stiffness values. First, a constant mass was placed at 0.33 m from the treadmill pivot point and the desired stiffness was changed from rigid ($k_t^d > 2$ MN/m) to 20 kN/m. A steady-state error (e_{ss}) of 7 N/m was obtained which is within the resolution of the system at that stiffness (see Fig. 6). Moreover, this error is still only a fraction of one percent as shown in Table I along with the rise time (t_r) and 1% settling time (t_s), averaged from three repeated trials.

Second, in order to verify that the controller is robust to nonlinearities not modeled in the linear system, we also tested the exact same controller, and gain values, with a step input of 56 kN/m. Results are shown in Table I. As seen in Fig. 4, the poles of the 20 and 56 kN/m systems are significantly far apart. However, with the closed-loop feedback, we achieve essentially zero steady-state error. This shows that the controller is robust enough to compensate for nonlinearities of the system. Therefore, the controller that we tuned to the 20 kN/m system will be

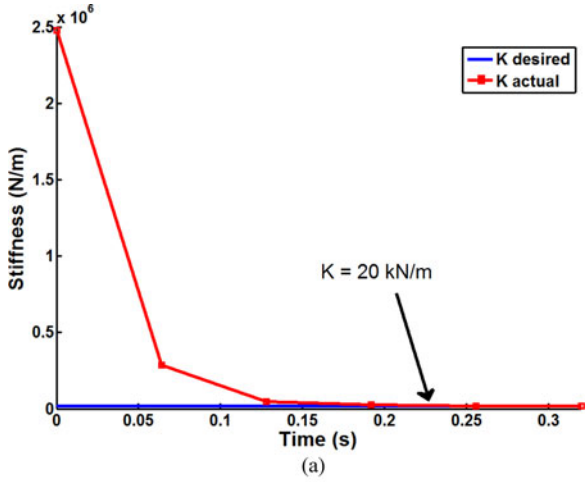

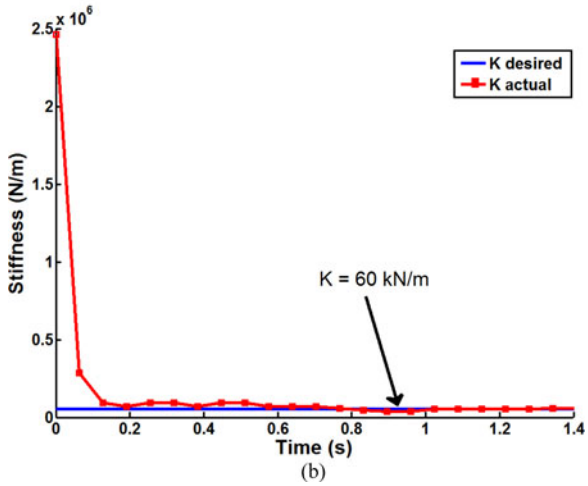

Fig. 6. Closed-loop response to a step input of desired stiffness of (a) 20 and (b) 56 kN/m.

TABLE I
CLOSED-LOOP RESPONSE

k_t^d (kN/m)	t_r (sec)	t_s (sec)	e_{ss} (%)
20	0.062	0.146	< 0.02
56	0.057	0.479	< 0.05

sufficient to achieve the desired stiffnesses within our range of interest.

In order to test the system in dynamic inputs and demonstrate the unique capabilities of the VST to create variable stiffness profiles, we created a reference sinusoidal input stiffness for the system to track. The signal oscillates about a mean of 20 kN/m at a frequency of 0.77 Hz. The mean value of 20 kN/m was selected to correspond to the linear model and the frequency of oscillation was chosen so that one period of the sinusoid would be approximately the duration of the stance phase. The system response is shown in Fig. 7. It can be seen that the actual stiffness profile matches the desired stiffness fairly well with some phase shift and attenuation. The magnitude attenuation is expected because it matches what the bode plot of the linear system (described previously) would suggest. The phase shift is

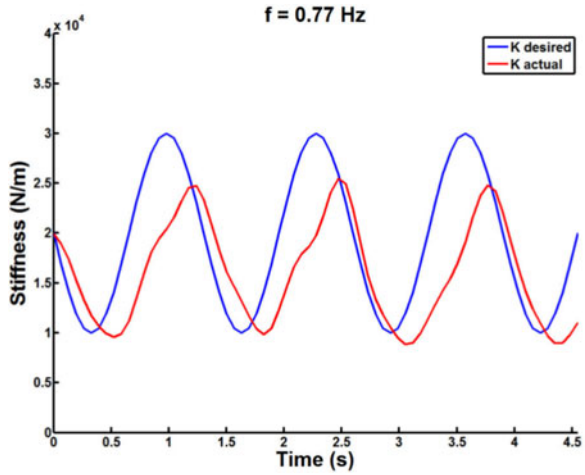

Fig. 7. Closed-loop system response to sinusoidal input.

approximately 50°, which is very close to what the Bode plot would indicate.

E. Additional Components

1) Optical Tracking System: A motion capture system (3D Investigator, Northern Digital) has been used for the purpose of tracking the foot position with respect to the treadmill surface. This optical-infrared tracking system also provides essential lower-limb and torso kinematic data from the subjects during experiments. This system has a 3-D accuracy of 0.4 mm and a resolution of 0.01 mm, which are adequate for our system.

2) Force Sensor Mat: Another approach to tracking the location of the subject's foot was implemented by placing an array of eight force sensing resistors beneath the treadmill belt. Whichever sensor is underneath the center of pressure of the foot will give the highest force reading. When two sensors give similar high force measurements, we can safely assume that the center of pressure is between the two sensors. So given that the sensor mat spans about 0.80 m, with our eight sensors, we have a spatial resolution of 0.05 m. Assuming that the average human foot length is about 0.235 m [23], this resolution is insufficient to know the location of the foot. The foot position is an important variable to know with high resolution because it is used as an input to calculate the corresponding linear track position that will create the proper apparent stiffness beneath the subject. Therefore, for these preliminary experiments, we used the high resolution motion tracking system instead.

However, it is anticipated that having a force mat sensor tracking system would be highly beneficial in a clinical setting. The lack of external devices and components would expedite rehabilitative procedures and decrease setup time significantly while also reducing unnatural stimulus from wearable hardware. The force sensor mat is shown in Fig. 1 (part C).

3) Split-Belt Treadmill: The VST employs a split-belt treadmill configuration in order to allow each belt to deflect different amounts. This will allow different force perturbations to be applied to each leg. The treadmill belts are supported at 0.70 m above the floor on a frame of steel tubing that permits each belt

to independently deflect downward to a maximum of 30° from the horizontal position. The adjustability of the treadmill stiffness is currently limited to only one belt, but can be applied to both sides by installing another variable stiffness mechanism. The split belt treadmill is shown in Fig. 1 (part D).

4) Treadmill Motor: A 1-hp variable speed DC motor (Anaheim Automation, Part Number: BDA-56C-100-90V-1800) drives the treadmill belts. We can obtain speeds of up to 1.85 m/s at a resolution of 7 mm/s. This includes the average-preferred walking speed of 1.2–1.4 m/s [16], [17], but can be slowed for individuals in therapy or rehabilitation applications. The treadmill motor is shown in Fig. 1 (part E).

5) Counterweight: One necessary component to ensure accurate control of treadmill stiffness is a counterweight system to eliminate moments created by the treadmill's weight. This is achieved by fastening a weighted slider at the precise location along a colinear beam which will induce an equal and opposite moment to that of the treadmill. This beam is attached to the side of the treadmill platform so that the counterweight system will cancel out the weight of the treadmill at any inclination of the treadmill. The counterweight is shown in Fig. 1 (part F).

6) Body Weight Support: Separate from the treadmill structure, there is a custom-built body weight support designed by LiteGait. By adjusting the height of the support system, we can choose to have full or partial body-weight support. This is an important capability to reduce ground reaction forces to allow more accurate control of force perturbations. In addition, the support increases safety and extends the system's capabilities to stroke patients and other individuals with decreased mobility and stability. Two load cells attached on the body-weight support harness are measuring the subject's weight supported by the mechanism from each side. The body weight support and the load cells are shown in Fig. 1 (parts G and H, respectively).

III. Results

In order to test the operation of the device and validate its performance, we conducted a few preliminary experiments with healthy subjects. Moreover, we show preliminary results related to the kinematic effect of varied body weight support and to unilateral stiffness perturbations.

A. Variable Body Weight Support

The first experiment was performed to see the kinematic effect of providing a different amount of body-weight support (or gravity compensation) while walking on a compliant surface. For the first experiment, two healthy males [age 23 ± 2.8 years, height 74 ± 28.3 in, weight 155 ± 4.2 lbs] walked on the treadmill moving at a comfortably slow speed of 0.55 m/s while the surface stiffness was maintained at 60 kN/m for the duration of the experiment. The subjects walked on the treadmill for at least 30 gait cycles. The value of stiffness was chosen to mimic other variable stiffness devices [13], [14], [20]–[22], while a treadmill stiffness of 60 kN/m resembles walking on a rubber platform [24]. For the first trial, no body weight support was provided, and it was controlled at approximately 30% for the second trial. The kinematic data were obtained using a motion capture system (3-D Investigator, Northern Digital) that was used to track five markers located at the torso, hip, knee, ankle, and toes of the subjects in order to calculate the joint angles throughout the gait cycle. The experimental protocol is approved by the Arizona State University Institutional Review Board (IRB ID#: STUDY00001001).

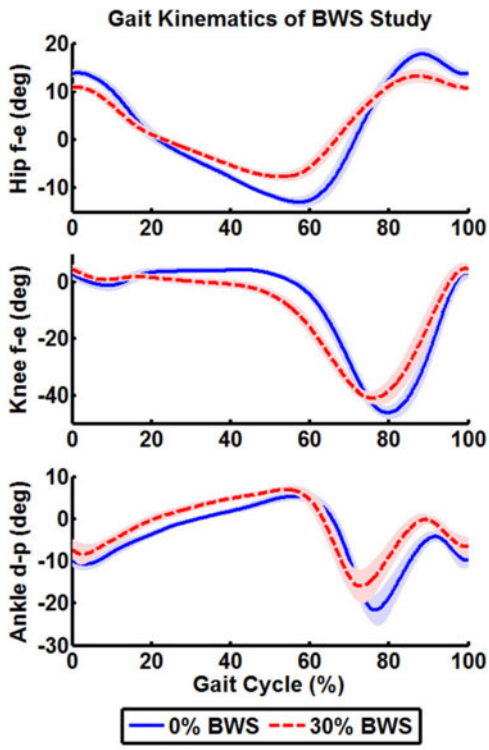

Fig. 8. Averaged kinematic data of hip flexion (+)–extension (-) [f–e], knee flexion (-)–extension (+) [f–e], and ankle dorsi (+)–plantar (-) flexion [d–p] with different levels of body weight support. Mean (solid lines) and standard deviations (shaded areas) values are shown. 0% corresponds to heel-strike.

The hip flexion-extension, knee flexion-extension, and ankle dorsi/plantar flexion for a representative subject are shown (mean and standard deviation across all gait cycles) in Fig. 8. The data is plotted as a function of the gait cycle percentage, where 0% corresponds to heel-strike, approximately 65% corresponds to toe-off, etc. As can be seen, the joint angle profiles (especially with 0% BWS) resemble that of normal gait [18], [25]. Therefore, our system did not alter the normal gait kinematics. However, all of the joint angles are significantly affected by increasing the body weight support. This is expected because more body weight support means that the subject will exert a smaller force on the treadmill surface which, for the same stiffness level, will deflect less leading to a shorter swing of the leg. Therefore, a narrower range of joint angles is expected as observed in Fig. 8. This is supported by the studies (eg., [26]) that have investigated the effect of body weight support on gait kinematics while walking on a rigid treadmill surface. We show similar results here while walking on a compliant surface. Further investigation of the effect of body weight support on gait kinematics is in the authors' future plans. However, it is out of the scope of this paper.

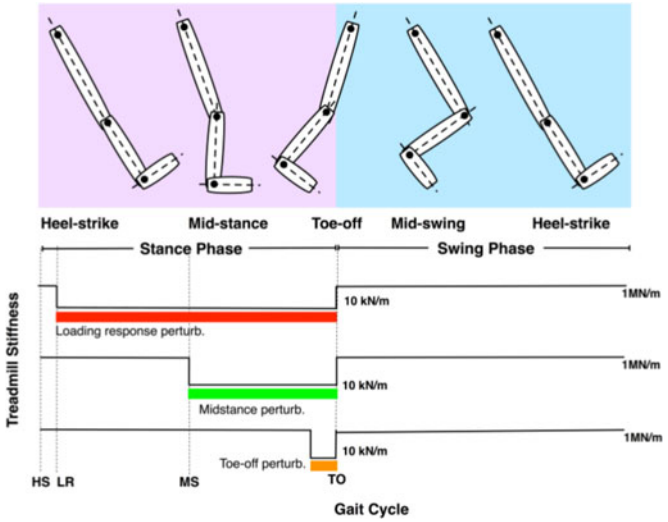

Fig. 9. Timing of unilateral perturbations.

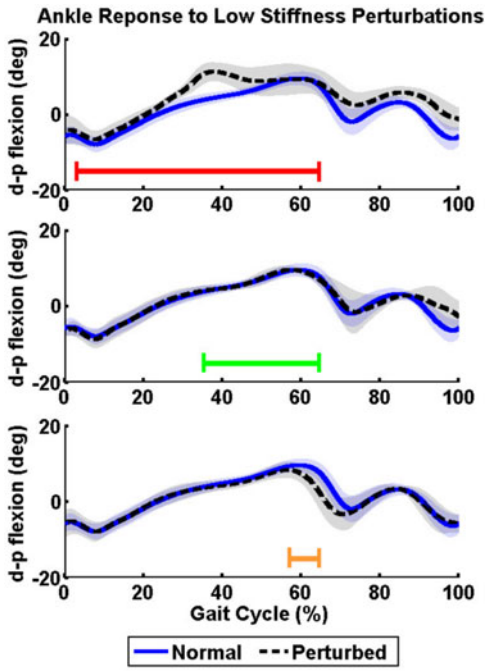

Fig. 10. Averaged kinematic data of ankle dorsi (+)–plantar (-) flexion [d–p] for normal (unperturbed) and perturbed walking. Mean (solid lines) and standard deviation (shaded areas) values are shown along with the timing of low stiffness perturbations (red, green, and orange lines).

B. Low Stiffness Perturbations

One of the unique capabilities of the VST is the ability to change the effective surface stiffness throughout the stance phase. An experiment with low stiffness perturbations was performed in order to demonstrate this feature. For this experiment, one healthy subject [age 24 years, height 73 in, weight 180 lbs] walked on the treadmill at a speed of 0.50 m/s with appoximately 20% body weight support and experienced three different perturbations. The treadmill stiffness was controlled to 1 MN/m, which is rigid, for a few gait cycles to collect the normal gait patterns of the subject. After a random number (n) of steps, where $n \in [3, 7]$, we immediately dropped the stiffness to 10 kN/m. The stiffness drop was done in one of three different stages of the left leg stance phase, 1) at loading response, 2) midstance, and 3) toe-off, and is shown in Fig. 9. For the perturbed gait cycle, one out of the three options was randomly selected. The low stiffness was maintained at the same value from the time of initiation until toe-off, after which the stiffness returned back to 1 MN/m for the next n number of steps. There were ten perturbations at each of the three locations during this experiment, and the right leg was always experiencing infinite stiffness. Kinematic data for the left leg were obtained using the same system as described in the first experiment previously.

The kinematic response of the ankle joint to these perturbations is shown in Fig. 10. Only the ankle joint is displayed for simplicity and because it was more affected by the stiffness perturbations than the knee and hip joints. The plots reveal that the timing and duration of the stiffness perturbations have a direct effect on the kinematic response of the ankle. Indeed, a perturbation beginning in the loading phase can evoke dorsiflexion while a perturbation in terminal stance creates greater plantarflexion. In addtion, the kinematic effect of the perturbation on the joint angle continues after the termination of the perturbation. This may be explained by attempts to recover balance and correct balance distribution in the swing phase. Future experiments will further investigate the effect of the timing of stiffness perturbations by utilizing the unique capability of the VST to create variable stiffness profiles.

IV. Conclusion

This paper presented the VST device that has been developed with several advantages over existing devices for gait research. The VST can alter the walking surface stiffness in real time, offering a wide range of available stiffness, from infinite stiffness (noncompliant walking surface) to as low as 61.7 N/m. The resolution of the controlled stiffness can reach a maximum of 0.038 N/m, while the effective stiffness can change from the maximum to the minimum in 0.13 s. All these characteristics make the VST a unique research platform. Unlike previous devices, the VST is capable of creating variable profiles of stiffness during an experiment and throughout the gait cycle.

This paper also identified the dynamics of our system and showed how the inherent nonlinearity of the system modifies the system open-loop poles. We implemented a feedback controller in order to eliminate any error from these nonlinear relationships so that the VST can be used to its fullest potential as a research tool in future experiments.

Apart from a unique research tool, the VST can be applied for gait rehabilitation. The ability to apply perturbations and regulate force feedback allow for the definition of rehabilitation protocols beyond the state of the art, where the interplay of the leg dynamics with a dynamic environment will play a major role. Moreover, the VST can be used as a simulation-testing device for biological and artificial walkers, when investigating

walking patterns and architectures in environments where variable stiffness is required.

REFERENCES

[1] R. af Klint, N. Mazzaro, J. B. Nielsen, T. Sinkjaer, and M. J. Grey, "Load rather than length sensitive feedback contributes to soleus muscle activity during human treadmill walking," *J. Neurophysiol.*, vol. 103, no. 5, pp. 2747–2756, 2010.

[2] M. J. Stephens and J. F. Yang, "Loading during the stance phase of walking in humans increases the extensor EMG amplitude but does not change the duration of the step cycle," *Exp. Brain Res.*, vol. 124, no. 3, pp. 363–370, 1999.

[3] J. F. Yang, M. J. Stephens, and R. Vishram, "Transient disturbances to one limb produce coordinated, bilateral responses during infant stepping," *J. Neurophysiol.*, vol. 79, no. 5, pp. 2329–2337, 1998.

[4] V. Dietz, A. Gollhofer, M. Kleiber, and M. Trippel, "Regulation of bipedal stance: Dependency on "load" receptors," *Exp. Brain Res.*, vol. 89, no. 1, pp. 229–231, 1992.

[5] V. Dietz, R. Müller, and G. Colombo, "Locomotor activity in spinal man: Significance of afferent input from joint and load receptors," *Brain*, vol. 125, no. 12, pp. 2626–2634, 2002.

[6] V. Dietz and J. Duysens, "Significance of load receptor input during locomotion: A review," *Gait Posture*, vol. 11, no. 2, pp. 102–110, 2000.

[7] M. Faist, C. Hoefer, M. Hodapp, V. Dietz, W. Berger, and J. Duysens, "In humans ib facilitation depends on locomotion while suppression of ib inhibition requires loading," *Brain Res.*, vol. 1076, no. 1, pp. 87–92, 2006.

[8] Y. P. Ivanenko, R. Grasso, V. Macellari, and F. Lacquaniti, "Control of foot trajectory in human locomotion: Role of ground contact forces in simulated reduced gravity," *J. Neurophysiol.*, vol. 87, pp. 3070–3089, 2002.

[9] M. J. Grey, J. B. Nielsen, N. Mazzaro, and T. Sinkjær, "Positive force feedback in human walking," *J. Physiol.*, vol. 581, no. 1, pp. 99–105, 2007.

[10] D. S. Marigold and A. E. Patla, "Adapting locomotion to different surface compliances: Neuromuscular responses and changes in movement dynamics," *J. Neurophysiol.*, vol. 94, no. 3, pp. 1733–1750, 2005.

[11] M. J. MacLellan and A. E. Patla, "Adaptations of walking pattern on a compliant surface to regulate dynamic stability," *Exp. Brain Res.*, vol. 173, no. 3, pp. 521–530, 2006.

[12] M. D. Chang, E. Sejdić, V. Wright, and T. Chau, "Measures of dynamic stability: Detecting differences between walking overground and on a compliant surface," *Human Movement Sci.*, vol. 29, no. 6, pp. 977–986, 2010.

[13] T. A. McMahon and P. R. Greene, "The influence of track compliance on running," *J. Biomech.*, vol. 12, no. 12, pp. 893–904, 1979.

[14] A. E. Kerdok, A. A. Biewener, T. A. McMahon, P. G. Weyand, and H. M. Herr, "Energetics and mechanics of human running on surfaces of different stiffnesses," *J. Appl. Physiol.*, vol. 92, no. 2, pp. 469–478, 2002.

[15] A. Jafari, N. G. Tsagarakis, and D. G. Caldwell, "AwAS-II: A new actuator with adjustable stiffness based on the novel principle of adaptable pivot point and variable lever ratio," in *Proc. IEEE Int. Robot. Autom. Conf.*, 2011, pp. 4638–4643.

[16] R. C. Browning, E. A. Baker, J. A. Herron, and R. Kram, "Effects of obesity and sex on the energetic cost and preferred speed of walking," *J. Appl. Physiol.*, vol. 100, no. 2, pp. 390–398, 2006.

[17] R. V. Levine and A. Norenzayan, "The pace of life in 31 countries," *J. Cross-Cultural Psychol.*, vol. 30, no. 2, pp. 178–205, 1999.

[18] J. Perry, "Gait analysis: Normal and pathological function," *APA*, 1992.

[19] A. Barkan, J. Skidmore, and P. Artemiadis, "Variable stiffness treadmill (VST): A novel tool for the investigation of gait," in *Proc. IEEE Int. Conf. Robot. Autom.*, 2014.

[20] C. T. Farley, H. H. Houdijk, C. Van Strien, and M. Louie, "Mechanism of leg stiffness adjustment for hopping on surfaces of different stiffnesses," *J. Appl. Physiol.*, vol. 85, no. 3, pp. 1044–1055, 1998.

[21] D. P. Ferris and C. T. Farley, "Interaction of leg stiffness and surface stiffness during human hopping," *J. Appl. Physiol.*, vol. 82, no. 1, pp. 15–22, 1997.

[22] D. P. Ferris, K. Liang, and C. T. Farley, "Runners adjust leg stiffness for their first step on a new running surface," *J. Biomech.*, vol. 32, no. 8, pp. 787–794, 1999.

[23] R. M. Pawar and M. N. Pawar, "Foot length—A functional parameter for assessment of height," *Foot*, vol. 22, no. 1, pp. 31–34, 2012.

[24] M. L. Daniel, P. Ferris, and C. T. Farley, "Running in the real world: Adjusting leg stiffness for different surfaces," *Proc. Biol. Sci.*, vol. 265, no. 1400, pp. 989–994, 1998.

[25] M. W. Whittle, *Gait Analysis: An Introduction*. Oxford, U.K.: Butterworth-Heinemann, 1996.

[26] A. J. Threlkeld, L. D. Cooper, B. P. Monger, A. N. Craven, and H. G. Haupt, "Temporospatial and kinematic gait alterations during treadmill walking with body weight suspension," *Gait Posture*, vol. 17, no. 3, pp. 235–245, 2003.

Jeffrey Skidmore received the B.S. degree in mechanical engineering from Brigham Young University, Provo, UT, USA, in 2013. He is currently working toward the Ph.D. degree in mechanical engineering at Arizona State University, Tempe, AZ, USA.

He is a Research Associate at the Human-Oriented Robotics and Controls Laboratory, Arizona State University. His research interests include rehabilitation robotics, control systems, system identification, neuromuscular control, and human locomotion.

Andrew Barkan is studying mechanical engineering at Barrett, the Honors College and Ira A. Fulton Schools of Engineering at Arizona State University (ASU), Tempe, AZ, USA. He is in the process of completing the 4+1 Graduate program at ASU to receive the M.S. degree in mechanical engineering.

He is a Research Assistant at the Human-Oriented Robotics and Controls Laboratory, Arizona State University. His research interests include rehabilitation robotics, mechanical design, control systems, human–robot interaction, brain–machine interfacing, and human augmentation technology.

Panagiotis Artemiadis received the Diploma and the Ph.D. degree in mechanical engineering from the National Technical University of Athens, Athens, Greece, in 2003 and 2009, respectively.

From 2009 to 2011, he was a Postdoctoral Research Associate at the Newman Laboratory for Biomechanics and Human Rehabilitation, Mechanical Engineering Department, Massachusetts Institute of Technology, Boston, MA, USA. Since 2011, he has been with Arizona State University, Tempe, AZ, USA, where he is currently an Assistant Professor in the Mechanical and Aerospace Engineering Department, and the Director of the Human-Oriented Robotics and Control Laboratory. His research interests include the areas of robotics, control systems, system identification, brain–machine interfaces, rehabilitation robotics, neurorobotics, orthotics, human motor control, mechatronics, and human–robot interaction.